Key stage and model of hydrocarbon accumulation of Ordovician reservoir in Gucheng area, Tarim Basin, China

You Zhang[1]*, Qiang Li[2], Yongbin Niu[3], Bin Li[4], Yanqing Shi[4] and Yumao Pang[5]

[1]PetroChina Hangzhou Research Institute of Petroleum Geology, Hangzhou, China, [2]Exploration and Development Research Institute, PetroChina Daqing Oilfield Company, Daqing, China, [3]College of Resource and Environment, Henan Polytechnic University, Jiaozuo, China, [4]College of Geosciences, China University of Petroleum (Beijing), Beijing, China, [5]College of Earth Science and Engineering, Shandong University of Science and Technology, Qingdao, China

The heterogeneity of deep carbonate reservoirs is strong, it is significant for exploration and development to clarify the key stages of oil and gas accumulation. Taking the Ordovician in the Gucheng area of Tarim Basin as an example, this paper systematically investigated the key stage and model of hydrocarbon accumulation using the data of the cores, thin sections, cathode luminescence tests, laser ablation U-Pb isotope geochronometry, bitumen reflectance, and fluid inclusion tests, and seismic interpretation. (1) The Tarim Basin mainly develops three sets of effective source rocks, namely the Cambrian Yuertusi Formation, Cambrian Moheershan Formation, and Mid-Lower Ordovician Heituwa Formation, which are concentrated in the slope-basin facies of eastern Tarim Basin. (2) The Gucheng area is located in a favorable paleo-structural position. The pathway system composed of vertical faults and lateral unconformities occurs in the paleo-uplift, which is critical for hydrocarbon migration and accumulation. (3) The laser in-situ U-Pb dating, distribution and genesis of reservoir bitumen, burial-thermal maturation history, and the homogenization temperature of fluid inclusions suggest that the multi-stage tectonic thermal events of the Caledonian and Hercynian stages result in key adjustment and modification to deep hydrocarbon accumulation. Due to magmatic hydrothermal activities, the Caledonian primary oil reservoir massively evolved into oil-cracking gas reservoirs and residual paleo-oil reservoirs. (4) The paleo tectonic-fluid effect plays an important factor controlling the development of the Ordovician reservoirs. The evolution of the hydrocarbon accumulation in Gucheng area can be divided into three stages, namely formation of primary oil and gas reservoirs, oil-cracking gas reservoirs, and adjustment, destruction and reforming of gas reservoirs. To sum up, the western and northern parts of the paleo-uplift with favorable source-reservoir-cap rock assemblage and less effects of hydrothermal activities are the favorable zones for hydrocarbon exploration in the Gucheng area, the Tarim Basin.

KEYWORDS

key accumulation stage, laser *in situ* U—Pb dating, hydrocarbon accumulation, Ordovician, Gucheng area

1 Introduction

Over the recent years, significant breakthroughs have been continuously made in carbonate rocks of the marine facies, which has become the major strategic field for sustainable development of deep hydrocarbon exploration in China (Jia and Pang 2013; Sun et al., 2013; Dong et al., 2020; Li H et al., 2022). The Ordovician of the Gucheng area, Tarim Basin, is deposited in the slope belt of the carbonate platform-basin transition. Compared with that of the carbonate platform facies in the basin, it presents more diverse reservoir types and is closer to the Cambrian–Lower Ordovician source rock. Therefore, the Gucheng area is considered to be one of the areas in the Tarim Basin with the best conditions for hydrocarbon generation and storage (Shen et al., 2018; Zhang et al., 2018; Hong et al., 2020; Zhang et al., 2021). By the end of 2021, PetroChina had made massive physical efforts of two-(2D) and three-(3D) dimensional seismic prospecting and drilling across its 1.9×10^4 km^2 lease area in the Gucheng area, and 18 prospecting wells have been drilled during the past 10 years. The exploration suffers from low success rates of prospecting wells, complex reservoirs, complicated conditions for hydrocarbon accumulation, the occurrence of pyrobitumen, and poor oil testing results due to poor reservoir porosity. A review of the whole exploration practice in eastern Tarim Basin reveals that hydrocarbon was discovered only in relatively limited areas, and no proven reserves have been submitted yet. Accordingly, doubts are raised regarding the exploration potential of the Lower Paleozoic carbonate rock of the Gucheng area of the eastern Tarim Basin.

Extensive work has been performed from numerous points of views, in terms of the stratigraphic sequence (Fan et al., 2007; Zhao et al., 2010; Lin et al., 2013; Zhao, 2015), lithofacies paleogeography (Feng et al., 2006; Feng et al., 2007; Liu et al., 2011; Zhang et al., 2015), structural–sedimentary evolution (Zhang et al., 2007; Han et al., 2009; Li Q et al., 2014; Wang G et al., 2014), characteristics and formation mechanisms of reservoir rocks (Zheng et al., 2016; Shao et al., 2019), and control factors of hydrocarbon accumulation and exploration fields (Cao et al., 2019; Lv et al., 2022; Tochukwu et al., 2022), and some commonly accepted basic understandings have been obtained. For instance, the hydrocarbon exploration in the Tarim Basin shall highlight the Gucheng area with a good source–reservoir rock configuration. However, the specific hydrocarbon accumulation conditions of the key blocks and key risk exploration fields remain controversial, and the previous understanding can no longer meet the requirement of risk exploration (Hou et al., 2020). The deep carbonate rocks have undergone multi-stage transformation, and it is difficult to accurately determine the reservoir formation process by relying on the traditional oil and gas reservoir formation research methods and technologies. Previous research shows that the effective combination of various elements, such as the source rock, reservoir rock, cap rock, migration pathway, and trap, is the key factor to hydrocarbon accumulation (Zhao et al., 2006; Zhang et al., 2011a; Li J et al., 2022; Richardson et al., 2022). In this paper, the formation period of carbonate reservoirs in the study area is precisely determined by laser *in situ* U–Pb isotope dating technology. This research discusses the key stage and model of hydrocarbon accumulation of the Ordovician reservoir in the Gucheng area, from perspectives of source rock conditions, hydrocarbon migration pathways, formation mechanisms of reservoir rocks, and modification of tectonic thermal events. Also, the favorable exploration zones are evaluated according to lessons learned from failure wells and exploration practice. The aforementioned research results are expected to provide more reliable references for ultra-deep hydrocarbon exploration in the Tarim Basin and similar areas.
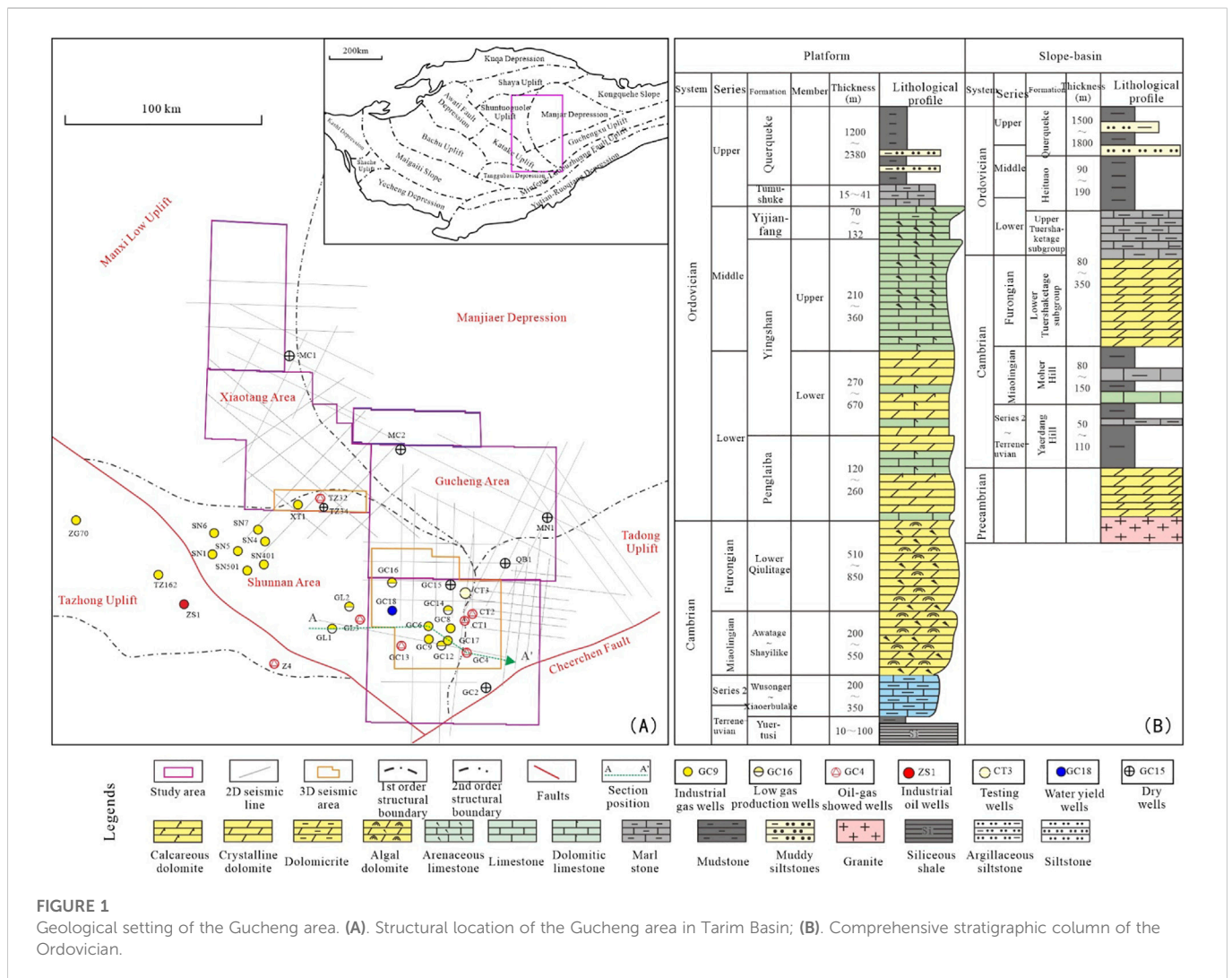
2 Geological setting

The Gucheng area is located in the east of the Tazhong uplift and southwestward of the Shunnan slope and northward of the Lunnan area. It connects with the Manjiaer sag and Tadong uplift. It is cut by the Cheerchen fault belt in the south (Figure 1A). In terms of geotectonics, the Gucheng lower uplift lies in the transition between the Tazhong and Tadong uplifts. It was formed during the middle Caledonian orogeny and finalized during the late Caledonian orogeny. Subsequently, it was further uplifted due to the Hercynian Northward compression and yet remained tectonically stable during the Indosinian–Himalayan movement (Dai et al., 1996; He et al., 2005; Gao, 2019).

A relatively complete stratigraphic association of the Sinian–Ordovician carbonate rocks develops in the Gucheng area, which is most of the carbonate platform and slope-basin deposition (Cai et al., 2013; Huang et al., 2013). The Cambrian–Ordovician in the study area presents an overall paleo-geographic framework characterized by a "platform in west and basin in east." In other words, the western part is the carbonate platform deposition, while the eastern part is the deposition of the platform margin and basin environments. The platform deposition is associated with a shallow water depth and development of the mound and shoal of the platform margin and the intra-platform grain shoal, of which the scales are controlled by the type and evolution of the platform. Moreover, the slope–basin deposition is found with a predominance of muddy sediments and considered favorable for development of high-quality source rocks (Figure 1B).

3 Samples and methods

The samples of this research are all collected from the 18 prospecting wells penetrating the Ordovician carbonate rock in the Gucheng area, Tarim Basin (Figure 1A). The conventional way to determine the relative sequence of diagenetic processes in research is mainly based on the contact relationships of minerals of varying stages revealed by the features observed in core observation and thin-section microscopy. The absolute age of minerals of a given stage can also be measured using the solution-based U–Pb isotope geochronometry (Woodhead et al., 2006; Woodhead and Pickering, 2012; Yuan et al., 2022). Nonetheless, these methods have the following disadvantages: first, the method based on the contact relationship among minerals of varying stages can only determine the relative sequence of diagenetic processes of a given sample, and in other words, it cannot directly determine the formation sequence of the same mineral component in different samples. Second, the solution-based U–Pb dating demands that samples to be tested have a sufficient content of U and Pb and consumes a large quantity of samples. However, the ancient marine carbonate rock is commonly associated with low content of U and Pb (Pickering et al., 2010) and small diameters of diagenetic components, resulting in failure to provide enough samples for

FIGURE 1
Geological setting of the Gucheng area. **(A)**. Structural location of the Gucheng area in Tarim Basin; **(B)**. Comprehensive stratigraphic column of the Ordovician.

tests (Hu et al., 2020; Li 2022), which restrains the application of the method. Over the past few years, these problems are all solved by the extensive application of laser ablation (LA)-based *in situ* U–Pb dating (Li Y. L et al., 2014; Coogan et al., 2016; Roberts et al., 2017; Roberts et al., 2020). After importing and digesting the foreign advanced technology, the CNPC Key Laboratory of Carbonate Reservoirs develops the LA-based *in situ* U–Pb dating specific to low U-content carbonate minerals. The test instrument is the LA-ICP-MS (Element XR), the reference materials are WC-1 (Roberts et al., 2017) and AHX-1 (Shen et al., 2019), and the isotope correction reference material is NIST 614 (Norman et al., 1996). The laser beam diameter is 100 μm, and the ablation frequency is 10 Hz. The main test procedure is presented below: (1) Prepare the sample target. (2) Determine the test zone according to the status of the target component (the LA target is marked in red. (3) Perform the LA and mass spectrometry across the test zone point by point. (4) Process the acquired test data and develop the Concordia diagram. This research targets the Ordovician of the Gucheng area in eastern Tarim and clarifies the key diagenetic stages *via* the comprehensive analysis based on the LA *in situ* U–Pb geochronometry assisted by the thin-section petrographic analysis and laser elemental surface

scanning to provide references for studying the heterogeneity of the Ordovician reservoirs in the Tarim Basin.

To illustrate the 3D distribution of pore-throats of the reservoir, the micro-nano-scale refined description is performed to produce the 3D pore-throat distribution model, using the high-precision micro-nano CT 3D imaging technology and e-core software for digital cores. The statistics of the parameters such as the pore-throat radius, shape factor, and spatial connectivity are obtained for pore-throat characterization.

The thin-section, cathode luminescence, and inclusion tests are finished in the CNPC Key Laboratory of Carbonate Reservoirs, and for the test methods, please refer to Pan et al. (2016).

4 Results and discussion

4.1 Source rocks

The facies of the slope-basin in eastern Tarim is the main distribution area of sources rocks in the Tarim Basin. In particular, it is claimed that the Gucheng area of eastern Tarim mainly develops the Cambrian Yuertusi Formation, Cambrian

FIGURE 2
History of burial–thermal maturation of a typical well in Gucheng area.
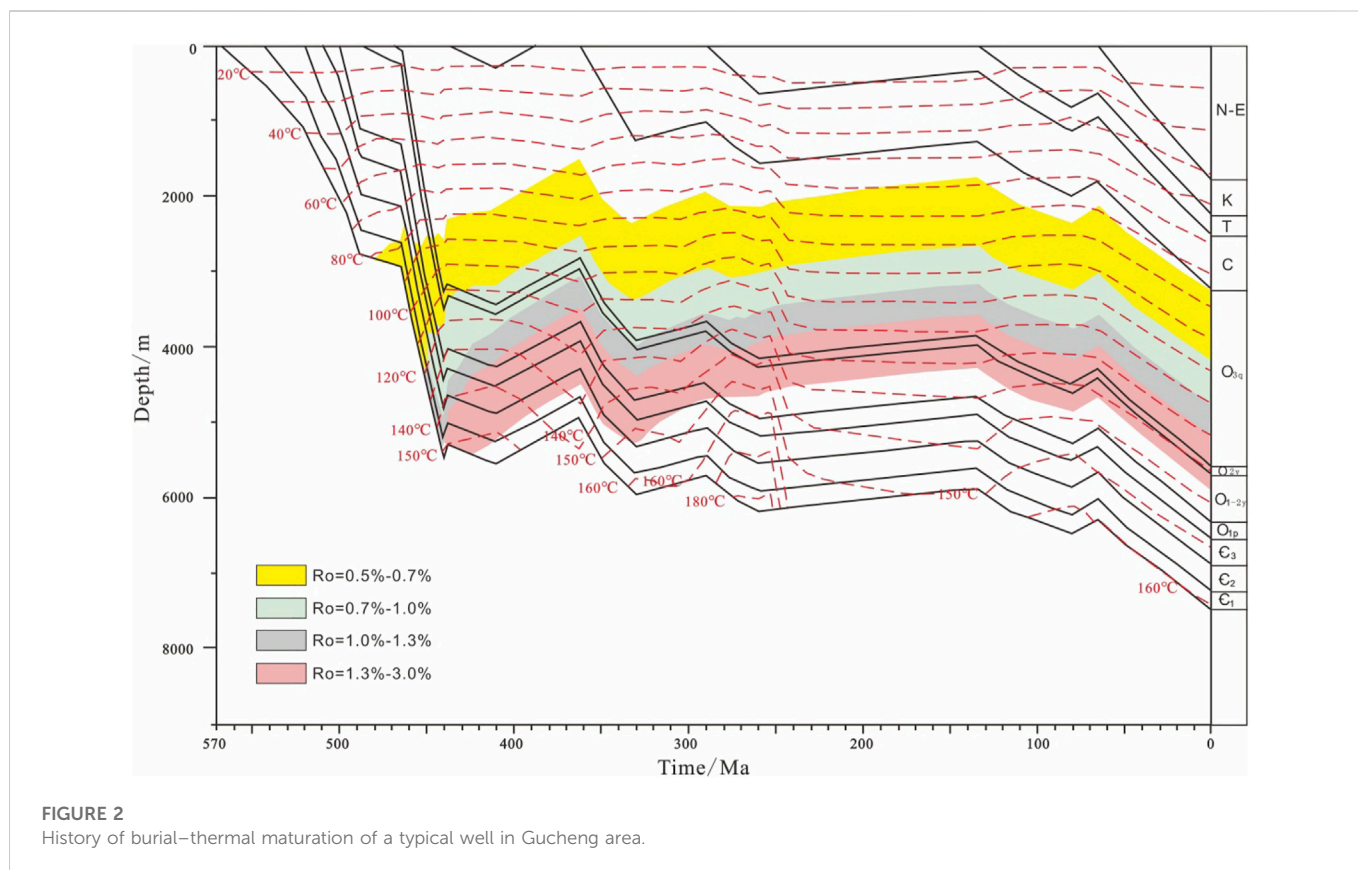
Moheershan Formation, and Mid-Lower Ordovician Heituwa Formation, three sets of effective source rocks, which mostly spread over the slope–basin facies belt of the eastern Gucheng uplift, eastern Tarim, after numerous studies reviewed the development of sources on the periphery of the Gucheng area in accordance with the field outcrops and newly acquired drilling and seismic data (Zhu et al., 2016; Guan et al., 2019).

The Terreneuvian source rock of the Cambrian mainly occurs in the Yuertusi Formation of the platform facies belt in the west and the Xidashan–Xishanbulake Formations of the basin facies belt in the east. Zhu et al. (2016); Li et al. (2020) performed geochemical analysis of over 10 outcrops of the Cambrian Yuertusi Formation in the Aksu area, and the black shale of the Yuertusi Formation presents TOC height up to 4%–16%, the highest among the discovered marine source rocks in China. Well Luntan-1 reveals that the black mudstone of the Cambrian Yuertusi Formation is 18 m thick, with TOC of 2.43%–18.48% (averaging 10.1%) and Ro of 1.5%–1.8%, and is considered a high-quality source rock (Yang et al., 2020). Wells TD1 and TD2 in the basin facies belt in the east also reveal this highly over-mature source rock, similar to that in the platform facies belt. The Miaolingian source rock of Cambrian mainly develops in the Moheershan Formation of the platform margin slope–basin facies belt in eastern Tarim, which is encountered in Wells TD2 and TD1 in the basin facies belt. It presents TOC of .51%–2.58% (averaging 1.60%) and Ro of 2.54% and is considered a medium–relatively high-quality source rock. The Mid-Lower Ordovician source rock is concentrated in the Heituwa Formation of eastern Tarim. It is the black shale of the basin facies deposition, with TOC of .50%–1.64% and Ro of 1.16%–2.10%, and

represents a medium–highly mature medium–high-quality source rock (Cao et al., 2019).

The analysis of the burial-thermal maturation history (Figure 2) shows that this source rock reaches the peak hydrocarbon generation and expulsion during the middle Caledonian stage. Massive gas generation *via* oil cracking of paleo-oil reservoirs occurs in the late Caledonian and late Hercynian stages. A large quantity of over-mature gas is generated during the Indosinian–Himalayan stage (Zhang et al., 2011a; Zhang et al., 2011b), which results in sufficient hydrocarbon supply of the Ordovician in the Gucheng area, Tarim Basin. The statistical overview of the source rock parameters is shown in Table 1.

4.2 Effective migration pathways

As for pathways for hydrocarbon migration, the network pathway system composed of vertical fault systems and lateral unconformities is found with extensive development across the paleo-uplift area, which serves as a good migration channel and effective pathway system of hydrocarbon migration and accumulation (Figure 3) (Mahmud et al., 2020; Shan et al., 2021). On one hand, multiple regional karst unconformities occur at the tops of the Yijianfang, Yingshan, and Penglaiba Formations and Furongian of Cambrian. Moreover, the effective reservoir thickness is large, and the lateral spreading of the reservoir rock is broadened and continuous. These are all in favor of hydrocarbons migrating along unconformities toward the higher position of the flank and accumulating in place. On the other hand, the Gucheng area is found with the development of multiple high-angle tensile normal faults penetrating downward the

TABLE 1 Source rock parameters.

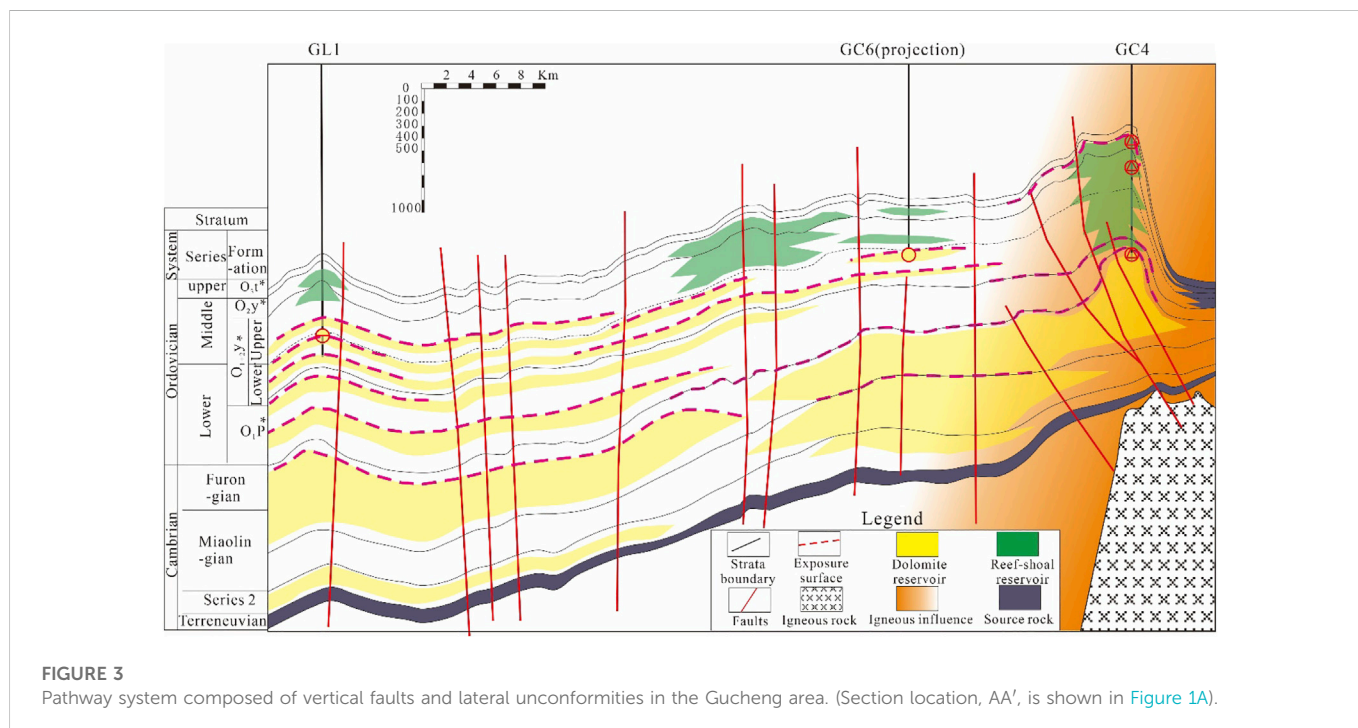| System	Series	Formation	TOC	Ro
Cambrian	Terreneuvian	Yuertusi Formation	2.43%–18.48%	1.5%–1.8%
	Miaolingian	Moheershan Formation	.51%–2.58%	2.54%
Ordovician	Mid-Lower	Heituwa Formation	.50%–1.64%	1.16%–2.10%

FIGURE 3
Pathway system composed of vertical faults and lateral unconformities in the Gucheng area. (Section location, AA′, is shown in Figure 1A).

Cambrian source rock and yet not cutting the overlying regional cap rocks (the Tumuxiuke Formation marlstone and the Queerqueke Formation mudstone). They provide effective vertical channels for hydrocarbon migration from the Cambrian source rock, while maintaining the integrity of the lithological–structural composite trap. Such faults are key factors for hydrocarbon accumulation in the Ordovician in the Gucheng area. In addition, due to invasion of igneous rocks, the paleo-oil reservoirs are baked and destructed, and yet such effects are lower down as further away from the invaded igneous rock (Figure 3). Tumuxiuke Fm is abbreviated as O_3t, Yijianfang Fm is abbreviated as O_2y, Yingshan Fm is abbreviated as $O_{1+2}y$, and Penglaiba Fm is abbreviated as O_1P. They all belong to the Ordovician.

4.3 Adjustment and modification of hydrocarbon accumulation by tectonic thermal events

The slope of the Gucheng area, Tarim Basin, lies at the east end of the Tazhong paleo-uplift, and the paleo-uplift background was established in the early Caledonian period. The southern part of this structural belt is relatively close to the Cheerchen fault, which is highly active during the late Caledonian stage and the late Permian,

associated with massive invasion of igneous rocks (Ran et al., 2008; Liu et al., 2010; Zhang et al., 2014). Such Permian massive magmatic invasion alters the geothermal field at that time (raised geothermal thermal gradients), and accordingly, the immature source rock on the periphery of the depression reaches the oil generation threshold, which promotes the hydrocarbon generation rate and quantity and accelerates the evolution of the source rock of the basin. As for the mature source rock in the basin, it is converted into over-mature source rock and enters the depletion stage of hydrocarbon generation (Ran et al., 2008; Liu et al., 2010; Zhang et al., 2014). The adjustment and modification of oil and gas reservoirs attributed to tectonic thermal events have critical influences on the formation and evolution of oil and gas reservoirs in terms of both materials and energy and complicate the hydrocarbon accumulation in the Ordovician of the Gucheng area.

4.3.1 Evidence from the laser *in situ* U–Pb dating

The Ordovician dolomite reservoir in the Gucheng area, Tarim Basin, has gone through superimposed modification of diagenetic fluids of multiple stages during its formation, which results in the high heterogeneity of the reservoir. To clarify the relative sequence of diagenetic processes of varying stages during the pore evolution of the Ordovician dolomite reservoir and their coupling relationships with pores of the reservoir, precisely determining the stages of the

TABLE 2 Components of tested samples and results of the laser *in situ* U–Pb dating.

Sample no.	Depth/m	Lithology	Tested component		U–Pb dating
			No.	Occurrence	
DQ17	6,058.22	Gray fine dolomite, with part of pore-vugs filled with calcite	①	Intergrowth-crystalline calcite	469 ± 22 Ma
			②	Surrounding rock fine dolomite	474.7 ± 7.5 Ma
DQ11	6,345.19	Dark gray fine–medium dolomite, with pore-vugs filled with coarse dolomite	③	Coarse dolomite	/*
			④	Surrounding rock fine–medium dolomite	346 ± 38 Ma

Remarks: "/" represents failure of the laser *in situ* U–Pb dating.

key diagenetic processes is critical. This research, based on the laser *in situ* U–Pb dating and laser *in situ* elemental surface scanning and imaging, performs a systematic isotope dating analysis for the three major textural constituents, the surrounding rock matrix, medium–coarse dolomite on the wall of the pore-vug, and calcite cement inside the pore-vug. The test results are shown in Table 2; Figure 4.

The fine dolomite of the surrounding rock and intergrowth-crystalline calcite in Sample DQ17 are tested (Figures 4A, B). The fine dolomite of the surrounding rock is dated to be 474.7 ± 7.5 Ma (Figure 4C), corresponding to the age of the Ordovician Yingshan Formation in the study area. The intergrowth-crystalline calcite is dated back to 469 ± 22 Ma (Figure 4D), which suggests that the Ordovician is subjected to the stage of calcium-rich hydrothermal fluids during the Caledonian orogeny and pore-vugs are filled with calcite. The fine–medium dolomite of the surrounding rock and the coarse dolomite in the pore-vug in Sample DQ11 are tested (Figure 4E). Owing to the extremely low content of uranium in the coarse dolomite of the fracture-vug, the laser *in situ* U-Pb dating fails. The fine–medium dolomite of the dark gray surrounding rock formed 346 ± 38 Ma (Figure 4F), indicating a stage of magnesium-rich hydrothermal fluids during the early Hercynian stage, with fractures and vugs filled by coarse calcite (Figures 5A–D), with high positive anomalies of the elements Y and Ce (Figures 5E, F). The filling of the coarse dolomite occurs after the formation of the fine–medium dolomite of the dark gray surrounding rock, which implies that the invasion of hydrothermal fluids migrates along the early Hercynian fault and the filling of coarse dolomite shall be slightly later than 346 Ma. The laser *in situ* U–Pb dating and the *in situ* elemental surface scanning and imaging show that the multi-stage tectonic thermal events during the Caledonian and Hercynian movement have essential adjustment and modification effects on deep hydrocarbon accumulation, accompanied by filling with saddle dolomite and calcite.

4.3.2 Evidence from the reservoir bitumen distribution and genesis

The drilling and core of wells in the study area reveal that from the Yijianfang Formation to the Upper Yingshan Formation and in the Penglaiba Formation occurs the over 1,000-m-thick bitumen paleo-oil reservoir. The reservoir bitumen extensively develops in the dissolution pore-vug (Figure 6A), stylolite and structural fracture (Figure 6B), inter-crystalline (dissolution) pore (Figure 6C), and mold (visceral foramen) pore (Figure 6D) of the Ordovician

carbonate reservoir of the paleo-uplift, and presents itself in filling forms of strips, grains, veins, and blocks (Li et al., 2019; Li et al., 2021a; Hou et al., 2020; Qie et al., 2021).

There have been many important understandings provided by previous studies on reservoir bitumen genesis. From the perspective of the genesis, the reservoir bitumen can be divided into three categories: pyrobitumen, biodegraded bitumen, and precipitated asphalt (Zhao et al., 2007). There are significant differences in morphology and maturity of bitumen of different geneses. Due to the high temperature and high pressure, the edge of the pyrobitumen is clearer, while the biodegraded bitumen and precipitated asphalt are often dispersed with blur edges and irregular shapes (Jacob, 1989). In addition, the reflectance of the pyrobitumen derived from crude oil cracking is much higher than those of precipitated asphalt and biodegraded bitumen (Hwang et al., 1998; Gao and Hu, 2002). The reflectance of pyrobitumen is generally above 4.0%–6.0%, and that of precipitated bitumen is usually .5%–1.5% (Ran et al., 2008).

The occurrence and reflectance of the reservoir's solid bitumen in the Gucheng area show that the solid bitumen is the pyrobitumen produced *via* the large-scale oil cracking of the original reservoirs affected by magmatic hydrothermal activities. Regardless of dolomite or limestone, the contained bitumen presents clear and straight edges, shapes of regular polygons, and vesicles developed on bitumen surfaces, which are typical features of pyrobitumen and indicate that the paleo-oil reservoir has experienced high-temperature baking. The solid bitumen reflectance is high, from 3.94%–7.75%. The measured reflectance of the same sample is highly variable and the bitumen is highly anisotropic, which implies intensive high thermal maturation. During the process of hydrothermal fluids flowing along faults and fractures, some special minerals, such as quartz, pyrite, fluorite, and bitumen (mainly pyrobitumen), precipitated, due to variation of pressure and temperature and interaction with surrounding rocks (Jin et al., 2006; Chen, 2008). In addition, the development of the siliceous hydrothermal filling also reflects the intensity of hydrothermal alteration (Figures 6E, F).

4.3.3 Evidence from homogenization temperatures of fluid inclusions

Fluid inclusions of the Ordovician reservoir rock in the Gucheng area mainly occur in the calcite vein, granular calcite, and crystalline quartz overgrowth and formed in the middle and late diagenesis. Observation identifies five types of fluid inclusions, namely, solid bitumen inclusion, hydrocarbon-containing brine
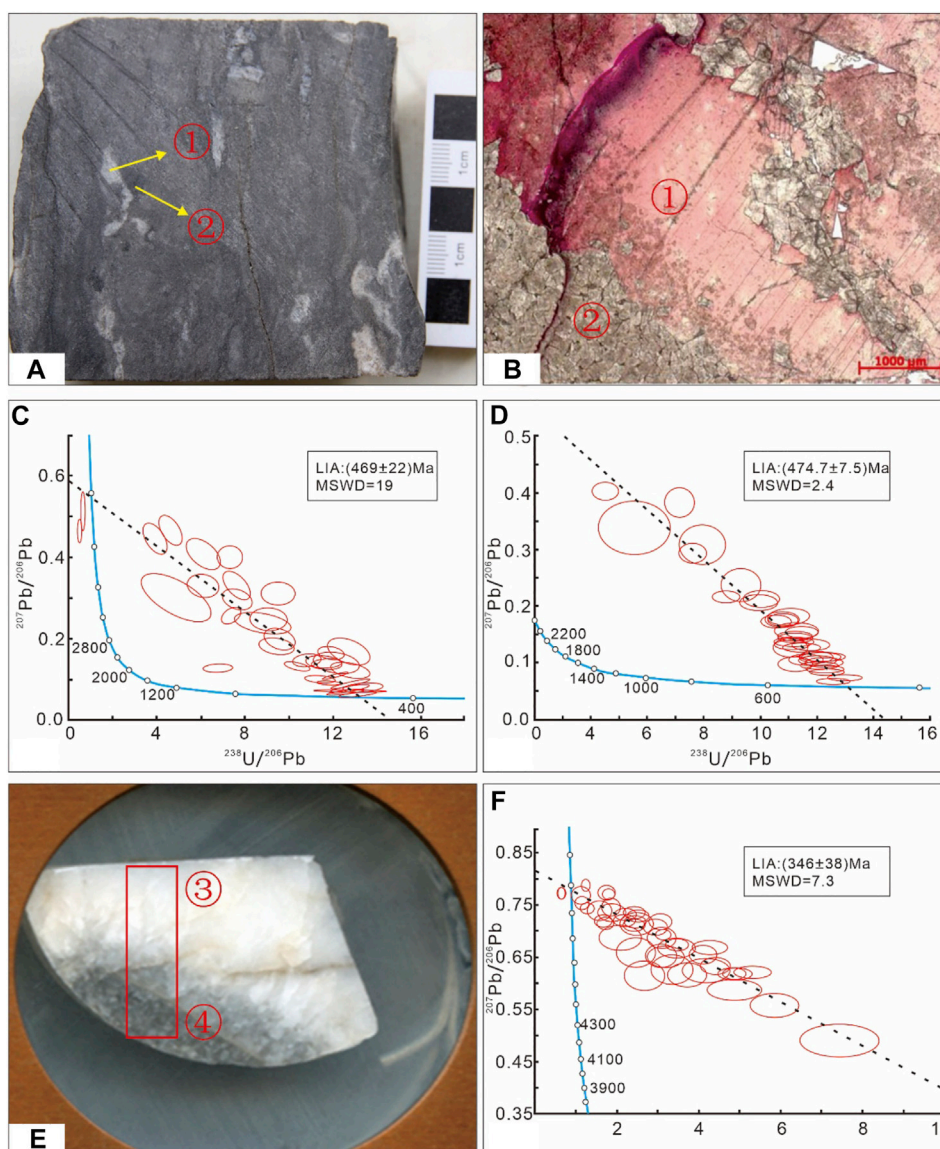
FIGURE 4
Characteristics of the Ordovician carbonate rock samples of the Tarim Basin (with marked sampling positions), and the U–Pb Concordia diagram. **(A)**. Two textural constituents of the ample tested in DQ17: ① the intergrowth-crystalline calcite in the pore-vug and ② the fine dolomite of the surrounding rock; **(B)**. Sampling positions for the thin section of sample DQ17: ① the intergrowth-crystalline calcite in the pore-vug and ② the fine dolomite of the surrounding rock; **(C)**. U–Pb isotope dating of the intergrowth-crystalline calcite in Sample DQ17; **(D)**. U–Pb isotope dating of the surrounding rock fine dolomite in Sample DQ17; **(E)**. Two tested textural constituents of Sample DQ11: ③ the coarse dolomite in the pore-vug and ④ the fine–medium dolomite in the surrounding rock; **(F)**. U–Pb isotope dating of the surrounding rock fine dolomite in Sample DQ11.

inclusion, two-phase brine inclusion, gas–liquid two-phase inclusion, and gaseous hydrocarbon inclusion. The bitumen inclusion is derived from the oil inclusion. Heavy hydrocarbons crack due to higher temperatures, and the inside pressure is raised to trigger bursting. Light hydrocarbons escape from the inclusion, and bitumen is left to form the bitumen inclusion, which is a direct evidence of oil emplacement. Gaseous hydrocarbon inclusions and gas–liquid two-phase inclusions may be derived from trapped cracking gas *via* oil cracking and also later charging of natural gas.

Identification and microthermometry have been performed for the hydrocarbon inclusions and associated brine inclusions in the Gucheng area (Table 3). The homogenization temperature of the organic fluid inclusion typically stands for the lowest temperature at the time the inclusion is captured. In other words, the temperature of the hydrocarbons migrates into the reservoir. Therefore, the peak temperature is indicative of the peak hydrocarbon migration. The analysis of oil stability of the marine facies reservoir in the platform-basin area of the Tarim Basin shows that 150°C is the threshold of crude oil cracking, and massive cracking is anticipated with a temperature over 200°C (Zhao et al., 2001), far higher than the formation temperature in cases of normal geothermal gradients. This suggests that the fluid temperature of the precipitated calcite vein is higher than the temperature of the surrounding rock, and thus such fluids are
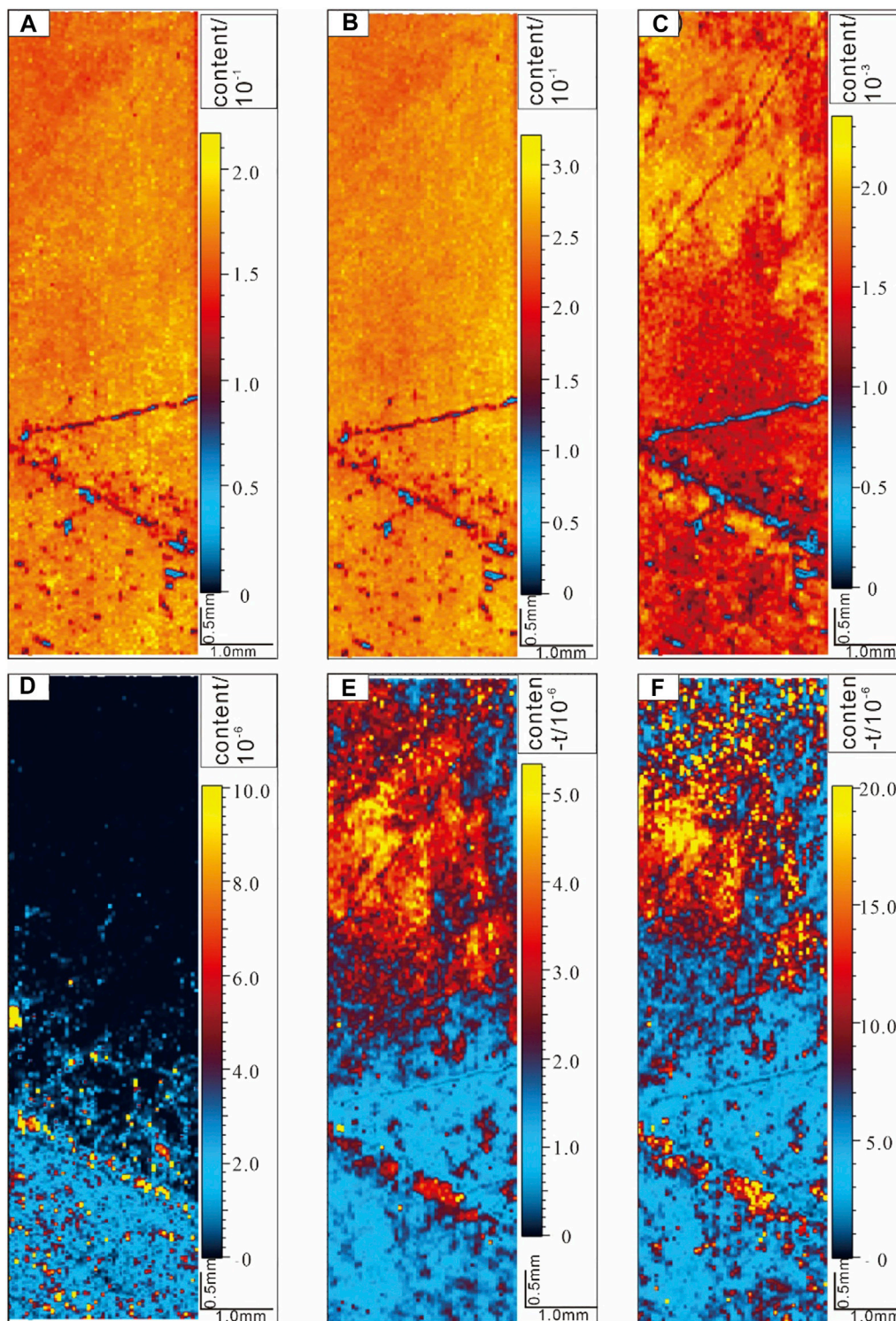
FIGURE 5
Element surface scanning images of Sample DQ11 in the Tarim Basin. **(A)**. Concentration of ^{25}Mg in horizontal distribution; **(B)** concentration of ^{43}Ca in horizontal distribution; **(C)** concentration of ^{55}Mn in horizontal distribution; **(D)** concentration of ^{238}U in horizontal distribution; **(E)** concentration of ^{89}Y in horizontal distribution; **(F)** concentration of ^{140}Ce in horizontal distribution.

typical deep hydrothermal fluids. Some geologists (Cai et al., 2008; Li K. K et al., 2010; Zhu et al., 2013) also validate the presence of hydrothermal fluids in the Lower Paleozoic of the Tarim Basin, according to the fact that the formation temperature of calcite is higher than the burial temperature.

4.3.4 Effective of paleo tectonic-fluid is a critical factor controlling the formation of hydrocarbon accumulation

The deep carbonate rock has gone through multi-stage variation of fluid-diagenetic environments of the tectonic, thermal, pressure,
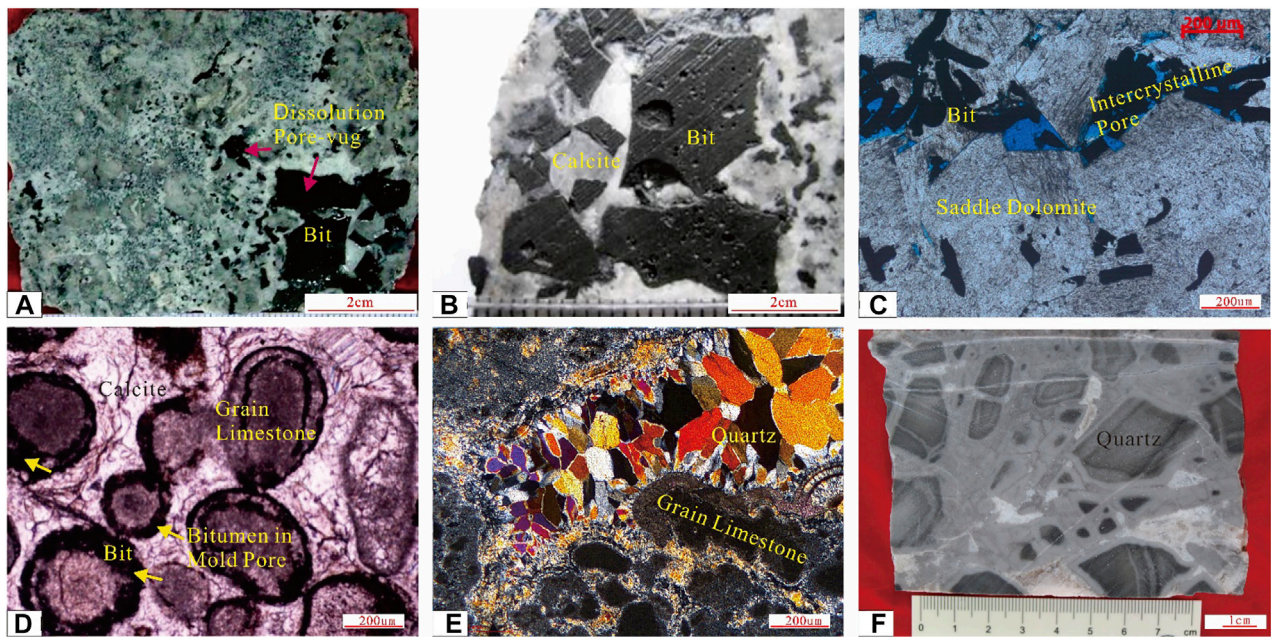
FIGURE 6
Occurrence of bitumen and siliceous hydrothermal metasomatism in the Ordovician carbonate reservoir in the Gucheng area. **(A)**. Bitumen in the dissolution pore-vug, Well GC4, Penglaiba Formation, 6,509 m; **(B)**. bitumen in the stylolite and structural fracture, with vesicles occurring on the bitumen surface, Well GC4, Yijianfang Formation, 5,597–5,600 m; **(C)** bitumen in the intercrystalline pore of dolomite, Well GC9, Yingshan Formation, 6,097.8 m; **(D)** bitumen in the mold pore, Well GC7, Yijianfang Formation, 5,662 m; **(E)** siliceous hydrothermal filling, Well GC15, Yingshan Formation, 6,356.7 m; **(F)** siliceous hydrothermal filling, Well GC14, Yingshan Formation, 6652 m.

and fluid regimes and time. The diagenesis is complicated, the diagenetic modification of multiple stages is superimposed, and the reservoir presents high heterogeneity (Chen et al., 2007; Zhao et al., 2012; Wang T. G et al., 2014; Li J et al., 2022). The temperature–pressure fields and fluid types are varied in different tectonic–burial–thermal maturation stages (Huang and Hou, 2001; Li Z et al., 2010; Fan et al., 2020; Li et al., 2021b). The Ordovician reservoir rock in the Gucheng area can be divided into two types, the Ordovician karst-dolomitization reservoir and the karst reef flat reservoir. In this research, the Ordovician karst-dolomitization reservoir is taken as an example to investigate the formation mechanisms of the complicated reservoir, such as the paleo-uplift setting, sedimentary facies, penecontemporaneous dissolution, and tectonic thermal events.

The Lower Ordovician karst-dolomitization reservoir in the Gucheng area, Tarim Basin, mainly occurs in the inner dolomitized shoal of the shallow-water ramp platform of the Lower Yingshan Formation and Penglaiba Formation. The reservoir space is dominated by residual pores, dissolution pore-vugs (Figure 7A), inter-crystalline or inter-granular (dissolution) pores (Figures 7B, C), and fractures. The reservoir samples mostly present medium–low porosity with medium–narrow throats, with high connectivity in local areas. The reservoir rocks are divided into the pore-vug type and fracture-vug type.

The CT comprehensive characterization of the Ordovician dolomite reservoir is shown in Figure 7D. CT scans of the reservoir pores show that the reservoir of the dolomitized shoal has higher micro-heterogeneity, manifested as the skewed distribution of pore-throats (uneven pore-vug diameter distribution from

.2 mm–10 mm), medium-narrow throats, a lower quantity of throats with uneven distribution of radii, and higher connectivity in local areas.

The development of the karst-dolomitization reservoir of the Lower Yingshan Formation and Penglaiba Formation is controlled by the paleo-uplift and sedimentary facies settings in the early stage. Moreover, the reservoir is subjected to the superimposed modification of the penecontemporaneous karstification, shallow burial dolomitization, and late faulting–hydrothermal activity. After a comprehensive analysis, it is claimed that the inner grain shoal of the shallow-water ramp serves as the basis for development of the dolomite reservoir, while the penecontemporaneous exposure dissolution is key to the formation of the reservoir. Pores are mostly inherited from the previous dolomitized shoal, while the faulting–hydrothermal modification creates important extra pores. (1) The shoal facies is the basis of the development of the dolomitized shoal reservoir, and the distribution of high-quality reservoirs is closely related to the inner dolomitized shoal of the shallow-water ramp. The reservoir dominated by the matrix pore-vug is mostly found in the fine–medium dolomite, which presents the phantom granular texture and along-bedding development of pores. This suggests that the dolomitized shoal is the basis for large-scale development of the reservoir, and the reservoir is a typical shoal-controlled reservoir. In addition, according to the analysis of the residual or restored original rock texture, the original rock of the crystalline dolomite is mostly grainstone of the shoal facies. The inter-granular (crystalline) pores of the dolomitized shoal deposition are the main reservoir space, and the sparry grainstone and wackestone are tight with fewer pores. (2) The

TABLE 3 Homogenization temperatures of brine inclusions in minerals filling the fracture-vug of the Ordovician of the Gucheng area, Tarim Basin. Liquid hydrocarbon inclusion is abbreviated as LHI. Solid bitumen inclusion is abbreviated as SBI. Gas–liquid two-phase inclusion is abbreviated as GLI. Gaseous hydrocarbon inclusion is abbreviated as GHI. Brine inclusion is abbreviated as BI.

Sample no.	Host mineral	Inclusion type	Color and shape	Test spots	Homogenization Temperature/°C		
					Max	Min	Average
Sygc001	Early fracture-vug calcite	LHI or SBI	Light blue fluorescence, irregular	11	116	123	118
Sygc002	Calcite vein	LHI or SBI	Light blue fluorescence, irregular	6			
Sygc003	Late calcite filling of pore-vugs and calcite vein	GLI	Oval and round	13	140	163	152
Sygc004	Quartz in karst vugs	GLI	Oval and round	9			
Sygc005	Recrystallization quartz overgrowth	GHI and GLI	Rectangular, oval, round, and irregular	7	167	185	171
Sygc006	Calcite vein	GHI and GLI	Rectangular, oval, round, and irregular	10			
Sygc007	Calcite vein	GHI and BI	Oval and irregular	11	150	210	203
Sygc008	Late calcite filling of fracture-vugs	GHI and BI	Oval, rectangular, and irregular	9	153	210	207

penecontemporaneous exposure dissolution is key to the formation of pores. The systematic coring over 100 m in Well GC601 reveals that the cored interval has over 30 exposure karst surfaces associated with extensive geopetal textures and vadose silt zones. The pore-vug interval mainly occurs in the dolomitized shoal below the top exposure surface of the high-frequency cycle, representing a typical penecontemporaneous fabric-selective dissolution and providing flow channels for dolomitization fluids in the later shallow-burial stage. (3) The dolomite reservoir mainly presents itself along the permeable shoal, fault, and unconformity surface. Pores are mostly the previous pores that are inherited and preserved. The samples are generally seen with brown luminescence under the cathode ray, and some crystals present bright red rims (Figure 7E), which indicates that the dolomite of the study area is mainly the burial metasomatism genesis, with late hydrothermal modification in local areas. The hydrothermal fluids derived from deeper layers serve as the diagenetic media for the saddle dolomite. From the perspective of the dissolution–precipitation of minerals with material balance and varying temperature and pressure conditions, the dissolution and cementation are in unity of opposites. The end of the tectonic hydrothermal activity is often associated with fillings of siliceous hydrothermal fluids, saddle dolomite, and calcite (Figure 7F) (Jiao et al., 2011; Chen et al., 2012).

4.4 Hydrocarbon accumulation model and predicted favorable zones of the Ordovician in the Gucheng area, Tarim Basin

4.4.1 Hydrocarbon accumulation model

The overall paleo-geographic framework of the Ordovician in the Gucheng area, Tarim Basin, features the transition from the platform environment to the basin environment. The Ordovician is close to the main source rock, and the hydrocarbon generation and accumulation are characterized by the generation in the basin and storage in the platform. According to the staged basin structural evolution, burial–thermal maturation simulation, and analysis of the main control factors of hydrocarbon accumulation, the hydrocarbon accumulation of the ancient deep carbonate reservoir can be divided into three stages (Figure 8).

4.4.2 Prediction of favorable zones

Crude oil cracking of paleo-oil reservoirs to generate gas is an important way to form deep natural gas, and such cracking gas is the main target for natural gas exploration of highly over-mature marine carbonate reservoirs in China (Zhao et al., 2007; Wang et al., 2008; Song et al., 2021; Wang and Wang, 2021). The analysis of the main controlling factors of the hydrocarbon accumulation in the Gucheng area, Tarim Basin, and the corresponding hydrocarbon accumulation evolution model suggest that the crude oil of the paleo-oil reservoir is massively converted into pyrobitumen and natural gas. The phase transition of deep fluids results in more rigorous requirements of hydrocarbon accumulation. With respect to the hydrocarbon exploration of the Ordovician in the Gucheng area, Tarim Basin, the following principle is recommended. The Caledonian–Early Hercynian primary oil reservoir shall be searched in the upper Ordovician karst reef flat reservoir on the periphery of the depression, far away from igneous rock invasion. The Late Hercynian cracking gas reservoir shall mostly occur in the Lower
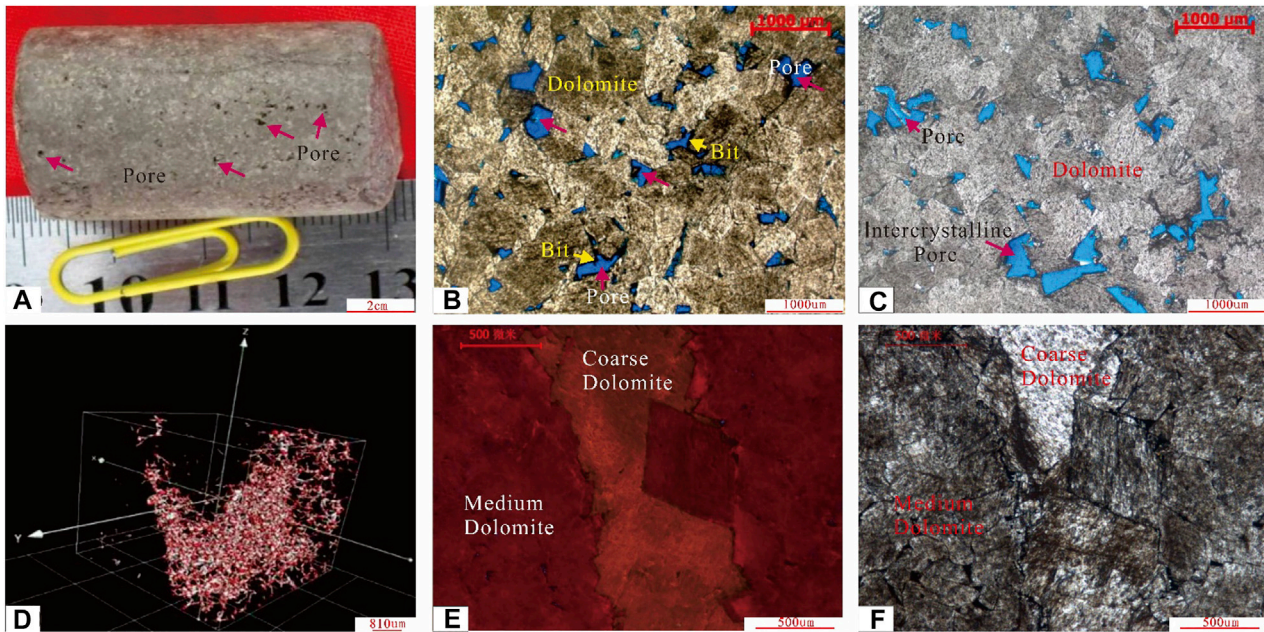
FIGURE 7
Reservoir space types and characteristics of the Ordovician karst-dolomitization reservoir in the Gucheng area, Tarim Basin. **(A)** Gray medium−coarse dolomite with dissolution pore-vugs (intergranular pore), Well GC13, the Yingshan Formation, 6,268 m; **(B)** medium−coarse dolomite with intercrystalline pores filled with bitumen, Well GC13, the Yingshan Formation, 6,268 m; **(C)** coarse dolomite with intercrystalline dissolution pores, Well GC9, the Yingshan Formation, 6,095.50 m; **(D)** pore-throat network model (with resolution of .9 um) with red representing pores and white representing throats, Well GC8, the Lower Yingshan Formation, 6,074.0 m; **(E)** medium−coarse dolomite with brown luminescence under the cathode ray and some crystals with red rims, Well GC14, the Yingshan Formation, 6,237.2 m; **(F)** medium−coarse dolomite with calcite hydrothermal filling, Well GC14, the Yingshan Formation, 6,237.2 m.

Ordovician karst-dolomitization reservoir along the paleo-oil reservoir and depression periphery. The exploration of the Himalayan gas reservoir shall focus on the large-scale gas generation of the liquid hydrocarbon scattered within the source rock during the highly over-mature stage. In summary, the western and northern parts of the paleo-uplift, with the premium source–reservoir–cap rock assemblage and fewer effects of faulting and tectonic hydrothermal activities, are the favorable exploration zones of hydrocarbon migration and accumulation.

5 Conclusion

1) The Ordovician oil and gas reservoir in the study area is attributed to the oil-cracking gas and late natural gas charging. The main controlling factors of the hydrocarbon accumulation in the Ordovician of the Gucheng area are the favorable paleo-structural setting, effective development of source rock, effective pathway system, modification of tectonic thermal events to hydrocarbon accumulation, and development conditions for high-quality reservoir rocks.

2) The paleo-tectonic-fluid effect is an important factor controlling the development of the reservoir rock and natural gas accumulation. The Ordovician karst-dolomitization reservoir is taken as an example to investigate the superimposed modification of various mechanisms, such as the paleo-uplift setting, sedimentary facies belt, penecontemporaneous dissolution, and tectonic thermal event. The grain shoal is the basis for the development of the dolomite reservoir, while the penecontemporaneous exposure dissolution is the key factor for reservoir formation. Pores are mostly inherited from the previous dolomitized shoal deposit, and faulting–hydrothermal modification creates important extra pores.

3) The formation and evolution of the Ordovician oil and gas reservoir in the Gucheng area, Tarim Basin, can be divided into three stages: the formation of primary oil and gas reservoirs, oil-cracking gas reservoirs, and adjustment, destruction, and reforming of gas reservoirs. The hydrocarbon accumulation model has the characteristics of multi-stage evolution.

4) Deep hydrothermal fluids migrate upward *via* faults, which is manifested as both destruction of the fault and vug-fracture reservoir system and constructive dissolution in different areas. The distribution mechanism for dissolution expansion and cementation still needs further investigation. Given the major challenge of poor continuity of high-quality reservoir and reservoir heterogeneity, it is recommended to quantitatively analyze the mechanisms of formation and preservation (dissolution and precipitation) of pores in the reservoir during the paleo–tectonic–hydrothermal process so as to reveal the distribution pattern and scale of high-quality reservoir rocks. In addition, given the small impedance difference between the low-porosity, low-permeability dolomite reservoir and tight limestone, it is suggested to enhance the seismic prediction technology for high-quality reservoirs, with the geological background of the study area taken into consideration. The future exploration practice shall target the northern and western parts of the
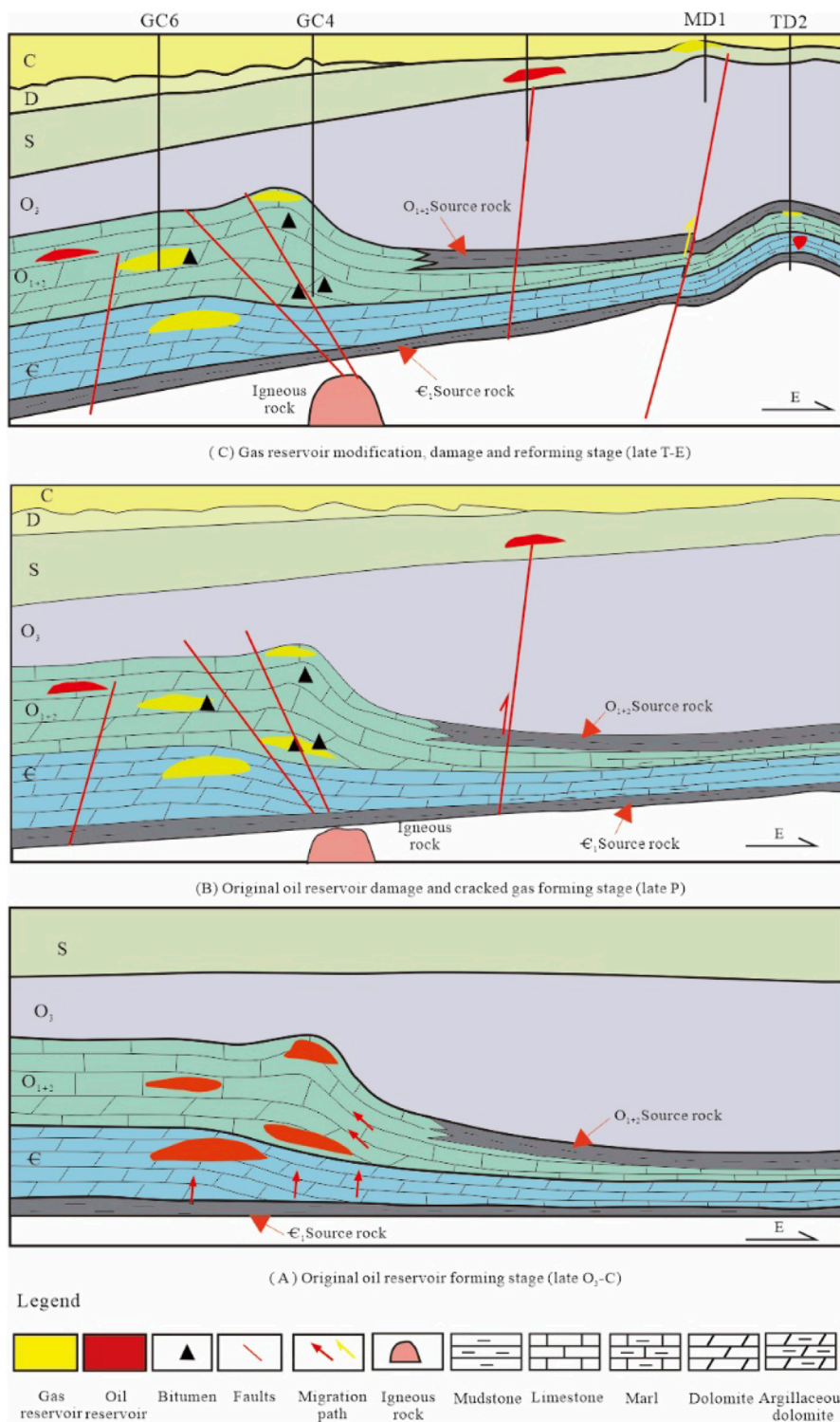
FIGURE 8
Hydrocarbon accumulation and evolution model in Gucheng area, Tarim Basin. **(A)** Formation of the primary oil and gas reservoir. The hydrocarbon generation of the three source rocks in the Cambrian–Ordovician of the Tarim Basin lasts until the late Hercynian stage, during which the primary oil reservoirs are formed, mostly in carbonate rock traps with some in the Silurian clastic rock. **(B)** Destruction and cracking of the primary oil reservoir. Due to the magmatic hydrothermal activities of multi-stage tectonic thermal events during the Caledonian and Hercynian stages, the primary oil reservoirs are subjected to oil cracking and the cracking gas reservoirs and residual paleo-oil reservoirs (or bitumen) are formed. **(C)** Adjustment, destruction, and reforming of gas reservoirs. The study area is tectonically stable after the Triassic. The trap integrity is maintained, and the preservation condition is good. The Cambrian–Ordovician source rock in the Manjiaer depression enters the hydrocarbon generation depletion stage, and part of crude oil is converted into natural gas *via* cracking, which forms condensate reservoirs. The dispersed residual organic matter in the source starts to generate gas at a large scale and forms the Himalayan gas reservoir, mostly occurring in traps related to the Himalayan movement.

Gucheng uplift that has a good source–reservoir–cap rock assemblage and is less affected by faulting and magmatic invasion.

Data availability statement

The original contributions presented in the study are included in the article/Supplementary Material, further inquiries can be directed to the corresponding author.

Author contributions

YZ, YN, and QL contributed in writing, reviewing, and editing; data curation; and writing—original draft preparation; BL, YS, and YP contributed in formal analysis, validation, and reviewing.

Funding

Acknowledgments

Conflict of interest

Author YN was employed by PetroChina Daqing Oilfield Company.

The remaining authors declare that the research was conducted in the absence of any commercial or financial relationships that could be construed as a potential conflict of interest.

Publisher's note

All claims expressed in this article are solely those of the authors and do not necessarily represent those of their affiliated organizations, or those of the publisher, the editors, and the reviewers. Any product that may be evaluated in this article, or claim that may be made by its manufacturer, is not guaranteed or endorsed by the publisher.

References

Cai, C. F., Li, K. K., Li, H. T., and Zhang, B. S. (2008). Evidence for cross formational hot brine flow from integrated 87Sr/86Sr, REE and fluid inclusions of the Ordovician veins in Central Tarim, China. *Appl. Geochem.* 23, 2226–2235. doi:10.1016/j.apgeochem.2008.03.009

Cai, X. Y., Dou, L. W., Jiang, H. S., Yu, T. X., and Cao, Z. C. (2013). Cambrian stratigraphic division and correlation in the eastern Tarim Basin. *J. Stratigr.* 37, 619. doi:10.19839/j.cnki.dcxzz.2013.04.081

Cao, Y. H., Wang, S., Zhang, Y. J., Yang, M., Yan, L., Zhao, Y. M., et al. (2019). Petroleum geological conditions and exploration potential of lower paleozoic carbonate rocks in Gucheng area, Tarim Basin, China. *Pet. Explor. Dev.* 46, 1165–1181. doi:10.1016/s1876-3804(19)60271-5

Chen, J. S., Li, Z., Wang, Z. Y., Tan, X. C., Li, L., and Ma, Q. (2007). Paleokarstification and reservoir distribution of ordovician carbonates in Tarim Basin. *Acta Sedimentol. Sin.* 25, 858–868. doi:10.14027/j.cnki.cjxb.2007.06.00

Chen, X., Zhao, W. Z., Zhang, L. P., Zhao, Z. J., Liu, Y. H., Zhang, B. M., et al. (2012). Discovery and exploration significance of structure-controlled hydrothermal dolomites in the Middle Permian of the central Sichuan Basin. *Acta Pet. Sin.* 33, 562–569. doi:10.7623/syxb201204004

Chen, D. Z. (2008). Structure-controlled hydrothermal dolomitization and hydrothermal dolomite reservoirs. *Oil Gas. Geol.* 29, 614–622. doi:10.11743/ogg20080510

Coogan, L. A., Parrish, R. R., and Roberts, N. M. (2016). Early hydrothermal carbon uptake by the upper oceanic crust: Insight from *in situ* U-Pb dating. *Geol.* 44, 147–150. doi:10.1130/G37212.1

Dai, J. X., Song, Y., and Zhang, H. F. (1996). Main factors controlling the foundation of medium-giant gas fields in China. *Sci. China (Series D).* 26 (6), 481–510. doi:10.1007/bf02878575

Dong, S., Zeng, L., Lyu, W., Xia, D., Liu, G., Wu, Y., et al. (2020). Fracture identification and evaluation using conventional logs in tight sandstones: A case study in the ordos basin, China. *Energy Geosci.* 1 (3-4), 115–123. doi:10.1016/j.engeos.2020.06.003

Fan, T. L., Yu, B. S., and Gao, Z. Q. (2007). Characteristics of carbonate sequence stratigraphy and its control on oil-gas in Tarim Basin. *Geosci.* 21, 57–65. doi:10.3969/j.issn.1000-8527.2007.01.006

Fan, C. H., Li, H., Qin, Q. R., He, S., and Zhong, C. (2020). Geological conditions and exploration potential of shale gas reservoir in Wufeng and Longmaxi Formation of southeastern Sichuan Basin, China. *J. Petrol. Sci. Eng.* 191, 107138. doi:10.1016/j.petrol.2020.107138

Feng, Z. Z., Bao, Z. D., Wu, B. M., Jin, Z. K., and Shi, X. Z. (2006). Lithofacies palaeogeography of the cambrian in Tarim area. *J. Palaeog.* 8, 427–439. doi:10.3969/j.issn.1671-1505.2006.04.001

Feng, Z. Z., Bao, Z. D., Wu, B. M., Jin, Z. K., Shi, X. Z., and Luo, A. R. (2007). Lithofacies palaeogeography of the ordovician in Tarim area. *J. Palaeog.* 9, 447–460. doi:10.7605/gdlxb.2007.05.001

Gao, Z. N., and Hu, H. Z. (2002). High pressure to the impact on the evolution of texture and compositon of natural bitumen. *Acta Sedimentol. Sin.* 20, 499–503. doi:10.14027/j.cnki.cjxb.2002.03.023

Gao, F. Q. (2019). Use of numerical modeling for analyzing rock mechanic problems in underground coal mine practices. *J. Min. Strata Control Eng.* 1 (1), 013004. doi:10.13532/j.jmsce.cn10-1638/td.2019.02.009

Guan, S. W., Zhang, C. Y., Ren, R., Zhang, S. C., Wu, L., Wang, L., et al. (2019). Early Cambrian syndepositional structure of the northern Tarim Basin and a discussion of Cambrian subsalt and deep exploration. *Petr. Explor. Dev.* 46, 1141–1152. doi:10.1016/s1876-3804(19)60269-7

Han, C. W., Ma, P. L., Zhu, D. X., Du, D. W., Xiao, J., and Liu, X. M. (2009). The tectonic characteristics and its evolution in the eastern Tarim Basin. *Xinjiang. Geotect. Metall.* 33, 131–135. doi:10.16539/j.ddgzyckx.2009.01.001

He, D. F., Jia, C. Z., Li, D. S., Zhang, C. J., Meng, Q. R., and Shi, X. (2005). Formation and evolution of polycyclic superimposed Tarim Basin. *Oil Gas. Geol.* 26, 64–77. doi:10.3321/j.issn:0253-9985.2005.01.010

Hong, D., Cao, J., Wu, T., Dang, S., Hu, W., and Yao, S. (2020). Authigenic clay minerals and calcite dissolution influence reservoir quality in tight sandstones: Insights from the central Junggar Basin, NW China. *Energy Geosci.* 1 (1-2), 8–19. doi:10.1016/j.engeos.2020.03.001

Hu, A. P., Shen, A. J., Liang, F., Zhao, J. X., Luo, X. Y., Feng, Y. X., et al. (2020). Application of laser *in-situ* U-Pb dating to reconstruct the reservoir porosity evolution in the Cambrian Xiaoerbulake Formation, Tarim Basin. *Oil Gas. Geol.* 41, 37–49. doi:10.11743/ogg20200104

Huang, S. J., and Hou, Z. J. (2001). Spatio-temporal variation of subsurface porosity and permeability and its influential factors. *Acta Sedimentol. Sin.* 19, 224–232. doi:10.14027/j.cnki.cjxb.2001.02.010

Huang, S. W., Zhang, Y., Zheng, X. P., Zhu, Q. F., Shao, G. M., Cao, Y. Q., et al. (2013). Types and characteristics of carbonate reservoirs and their implication on hydrocarbon exploration: A case study from the eastern Tarim Basin, NW China. *J. Nat. Gas Geoscience* 2, 73–79. doi:10.1016/j.jnggs.2017.02.001

Hwang, R. S., Teerman, S., and Carlson, R. (1998). Geochemical comparison of reservoir solid bitumens with diverse origins. *Org. Geochem.* 29, 505–517. doi:10.1016/S0146-6380(98)00078-3

Jacob, H. (1989). Classification, structure, Genesis and practical importance of natural solid oil bitumen ("migrabitumen"). *Int. J. Coal Geol.* 11, 65–79. doi:10.1016/0166-5162(89)90113-4

Jia, C. Z., and Pang, X. Q. (2013). Research processes and main development directions of deep hydrocarbon geological theories. *Acta Pet. Sin.* 36, 1457–1469. doi:10.7623/syxb201512001

Jiao, C. L., He, Z. L., Xing, X. J., Qin, H. R., He, B. Z., and Li, C. C. (2011). Tectonic hydrothermal dolomite and its significance of reservoirs in Tarim Basin. *Acta Petrol. Sin.* 27, 277–284. doi:10.1000-0569/2011/027(01)-0277-84

Jin, Z. J., Zhu, D. Y., and Hu, W. X. (2006). Geological and geochemical signatures of hydrothermal activity and their influence on carbonate reservoir beds in the Tarim Basin. *Acta Geol. Sin.* 80, 245–253. doi:10.3321/j.issn:0001-5717.2006.02.009

Li, H., Tang, H. M., Qin, Q. R., Zhou, J. L., Qin, Z. J., Fan, C. H., et al. (2019). Characteristics, formation periods and genetic mechanisms of tectonic fractures in the tight gas sandstones reservoir: A case study of xujiahe Formation in YB area, sichuan basin, China. *J. Petroleum Sci. Eng.* 178, 723–735. doi:10.1016/j.petrol.2019.04.007

Li, Y., Zhou, D., Wang, W., Jiang, T., and Xue, Z. (2020). Development of unconventional gas and technologies adopted in China. *Energy Geosci.* 1 (1-2), 55–68. doi:10.1016/j.engeos.2020.04.004

Li, H., Wang, Q., Qin, Q. R., and Ge, X. Y. (2021a). Characteristics of natural fractures in an ultradeep marine carbonate gas reservoir and their impact on the reservoir: A case study of the maokou Formation of the JLS structure in the sichuan basin, China. *Energy & Fuels* 35 (16), 13098–13108. doi:10.1021/acs.energyfuels.1c01581

Li, H., Peng, R., Du, W. S., Li, X. P., and Zhang, N. B. (2021b). Experimental study on structural sensitivity and intervention mechanism of mechanical behavior of coal samples. *J. Min. Strata Control Eng.* 3 (4), 043012. doi:10.13532/j.jmsce.cn10-1638/td.20210820.001

Li, H., Zhou, J. L., Mou, X. Y., Guo, H. X., Wang, X. X., An, H. Y., et al. (2022). Pore structure and fractal characteristics of the marine shale of the longmaxi Formation in the changning area, southern sichuan basin, China. *Front. Earth Sci.* 10, 1018274. doi:10.3389/feart.2022.1018274

Li, J., Li, H., Yang, C., Wu, Y. J., Gao, Z., and Jiang, S. L. (2022). Geological characteristics and controlling factors of deep shale gas enrichment of the Wufeng-Longmaxi Formation in the southern Sichuan Basin, China. *Lithosphere* 2022, 4737801. doi:10.2113/2022/4737801

Li, K. K., Cai, C. F., He, H., Jiang, L., Cai, L. L., Xiang, L., et al. (2010). Origin of palaeowaters in the Ordovician carbonates in Tahe oilfield, Tarim Basin: Constraints from fluid inclusions and Sr, C and O isotopes. *Geofl.* 11, 71–86. doi:10.1111/j.1468-8123.2010.00312.x

Li, Q., Parrish, R. R., Horstwood, M. S. A., and McArthur, J. M. (2014). U-Pb dating of cements in Mesozoic ammonites. *Chem. Geol.* 376, 76–83. doi:10.1016/j.chemgeo.2014.03.020

Li, Y. L., Wang, X. D., Sun, X. D., Tian, X. B., Jin, Z. L., and Yan, B. (2014). Structural evolution and favorable exploration direction for Gucheng low uplift. *Pet. Geol. Oilf. Dev. Daqing.* 33, 97–102. doi:10.3960/J.ISSN.1000-3754.2014.05.016

Li, Z., Huang, S. J., Liu, J. Q., Cai, C. F., Li, Y. J., Li, K. K., et al. (2010). Buried diagenesis, structurally controlled thermal fluid process and their effect on ordovician carbonate reservoirs in tahe, Tarim Basin. *Acta Sedimentol. Sin.* 28, 969–979. doi:10.14027/j.cnki.cjxb.2010.05.02

Li, H. (2022). Research progress on evaluation methods and factors influencing shale brittleness: A review. *Energy Rep.* 8, 4344–4358. doi:10.1016/j.egyr.2022.03.120

Lin, C. S., Yang, H. J., Cai, Z. Z., Yu, B. S., Chen, J. Q., Li, H., et al. (2013). Evolution of depositional architecture of the ordovician carbonate platform in the Tarim Basin and its response to basin processes. *Acta Sedimentol. Sin.* 31, 907–919. doi:10.14027/j.cnki.cjxb.2013.05.017

Liu, C. X., Li, T. G., and Liu, C. X. (2010). Deep fluid activity in Central Tarim Basin and its heating effects on hydrocarbon generation and accumulation. *J. Jilin Univ. Earth Sci. Ed.* 40, 279–285. doi:10.13278/j.cnki.jjuese.2010.02.019

Liu, W., Zhang, G. Y., Pan, W. Q., Deng, S. H., and Li, H. H. (2011). Lithofacies palaeogeography and sedimentary evolution of the Cambrian in Tarim area. *J. Palaeog.* 13, 529–538. doi:10.7605/gdlxb.2011.05.007

Lv, J., Yin, S., Sun, Y. H., Liu, L. J., Li, W. Z., Tao, D. S., et al. (2022). A new method for predicting injection multiples of extreme displacement in waterflood reservoirs. *Energy Geosci.* 4 (3), 465–472. doi:10.1016/j.engeos.2022.01.002

Mahmud, H., Hisham, M., Mahmud, M., Leong, V., and Shafiq, M. (2020). Petrophysical interpretations of subsurface stratigraphic correlations, Baram Delta, Sarawak, Malaysia. *Energy Geosci.* 1 (3-4), 100–114. doi:10.1016/j.engeos.2020.04.005

Norman, M. D., Pearson, N. J., Sharma, A., and Griffin, W. L. (1996). Quantitative analysis of trace elements in geological materials by laser ablation ICPMS: Instrumental operating conditions and calibration values of NIST glasses. *Geost. Newsl.* 20, 247–261. doi:10.1111/j.1751-908X.1996.tb00186.x

Pan, L. Y., Shen, A. J., Shou, J. F., Hu, A. P., and Wei, D. X. (2016). Fluid inclusion and geochemical evidence for the origin of sparry calcite cements in Upper Permian Changxing reefal limestones, eastern Sichuan Basin (SW China). *J. Geochem. Explor.* 171, 124–132. doi:10.1016/j.gexplo.2016.01.006

Pickering, R., Kramers, J. D., Partridge, T., Kodolayi, J., and Pettke, T. (2010). U-Pb dating of calcite–aragonite layers in speleothems from hominin sites in South Africa by MC-ICP-MS. *Quat. Geochronol.* 5, 544–558. doi:10.1016/j.quageo.2009.12.004

Qie, L., Shi, Y. N., and Liu, J. G. (2021). Experimental study on grouting diffusion of gangue solid filling bulk materials. *J. Min. Strata Control Eng.* 3 (2), 023011. doi:10.13532/j.jmsce.cn10-1638/td.20201111.001

Ran, Q. G., Cheng, H. G., Xiao, Z. Y., Ye, X. L., Wu, D. M., and Sang, H. (2008). Tectonic thermal event and its influence on cracking of crude oil in Eastern Tarim Basin. *Geosci.* 22, 541–548. doi:10.3969/j.issn.1000-8527.2008.04.008

Richardson, M., Abraham, A., Fabio, T., and Anthony, I. N. (2022). Physical properties of sandstone reservoirs: Implication for fluid mobility. *Energy Geosci.* 4 (3), 349–359. doi:10.1016/j.engeos.2022.06.001

Roberts, N. M., Rasbury, E. T., Parrish, R. R., Smith, C. J., Horstwood, M. S. A., and Condon, D. J. (2017). A calcite reference material for LA-ICP-MS U-Pb geochronology. *Geochem. Geophy. Geosy.* 18, 2807–2814. doi:10.1002/2016GC006784

Roberts, N. M. W., Drost, K., Horstood, M. S. A., Condon, D. J., Chew, D., Drake, H., et al. (2020). Laser ablation inductively coupled plasma mass spectrometry (LA-ICP-MS) U-Pb carbonate geochronology: Strategies, progress, and limitations. *Geochronol.* 2, 33–61. doi:10.5194/gchron-2-33-2020

Shan, S. C., Wu, Y. Z., Fu, Y. K., and Zhou, P. H. (2021). Shear mechanical properties of anchored rock mass under impact load. *J. Min. Strata Control Eng.* 3 (4), 043034. doi:10.13532/j.jmsce.cn10-1638/td.20211014.001

Shao, H. M., Lu, X., Gao, B., Hong, S. X., Pan, H. F., Xu, Z. Y., et al. (2019). Geochemical analyzing technique of the microzone's normal position and its application: A case study on the diagenetic evolution of the carbonate reservoir in Gucheng area. *Pet. Geo. Oilf. Dev. Daqing.* 38, 160–168. doi:10.19597/J.ISSN.1000-3754.201907005

Shen, A. J., Fu, X. D., Zhang, Y., Zheng, X. O., Liu, W., Shao, G. M., et al. (2018). A study of source rocks & carbonate reservoirs and its implication on exploration plays from Sinian to Lower Paleozoic in the east of Tarim Basin, northwest China. *Nat. Gas. Geosci.* 29, 1–16. doi:10.11764/j.issn.1672-1926.2017.08.019

Shen, A. J., Hu, A. P., Cheng, T., Liang, F., Pan, W. Q., Feng, X. Y., et al. (2019). Laser ablation *in situ* U-Pb dating and its application to diagenesis-porosity evolution of carbonate reservoirs. *Petr. Explor. Dev.* 46, 1127–1140. doi:10.1016/s1876-3804(19)60268-5

Song, J. F., Lu, C. P., Li, Z. W., Ou, Y. G. C., Cao, X. M., and Zhou, F. L. (2021). Characteristics of stress distribution and microseismic activity in rock parting occurrence area. *J. Min. Strata Control Eng.* 3 (4), 043518. doi:10.13532/j.jmsce.cn10-1638/td.20210607.002

Sun, L. D., Zou, C. N., Zhu, R. K., Zhang, Y. H., Zhang, S. C., Zhang, B. M., et al. (2013). Formation, distribution and potential of deep hydrocarbon resources in China. *Pet. Explor. Dev.* 40, 687–695. doi:10.1016/s1876-3804(13)60093-2

Tochukwu, N., Manoj, M., and Suame, A. (2022). Reconnaissance investigation of geothermal resources in parts of the Middle Benue Trough, Nigeria using remote sensing and geophysical methods. *Energy Geosci.* 4 (3), 360–371. doi:10.1016/j.engeos.2022.06.002

Wang, J., and Wang, X. L. (2021). Seepage characteristic and fracture development of protected seam caused by mining protecting strata. *J. Min. Strata Control Eng.* 3 (3), 033511. doi:10.13532/j.jmsce.cn10-1638/td.20201215.001

Wang, T. S., Geng, A. S., Xiong, Y. Q., Liao, Z. W., and Li, X. (2008). Kinetic simulation study on generation of gaseous hydrocarbons from the pyrolysis of marine crude oil and its asphaltene in Tarim Basin. *Acta Pet. Sin.* 29, 167–172. doi:10.3321/j.issn:0253-2697.2008.02.002

Wang, G., Fan, T. L., and Liu, H. L. (2014). Characteristics and evolution of ordovician carbonate platform marginal facies in tazhong-gucheng area. *Tarim. Basin. Geosci.* 28, 995–1007. doi:10.3969/j.issn.1000-8527.2014.05.015

Wang, T. G., Song, D. F., Li, M. J., Yang, C. Y., Ni, Z. Y., Li, H. L., et al. (2014). Natural gas source and deep gas exploration potential of the Ordovician Yingshan Formation in the Shunnan-Gucheng region, Tarim Basin. *Oil Gas. Geol.* 35, 753–762. doi:10.11743/ogg20140602

Woodhead, J., and Pickering, R. (2012). Beyond 500 ka: Progress and prospects in the U-Pb chronology of speleothems. *Quat. Int.* 540, 540. doi:10.1016/j.quaint.2012.08.1895

Woodhead, J., Hellstrom, J., Maas, R., Drysdale, R., Zanchetta, G., Devine, P., et al. (2006). U-Pb geochronology of speleothems by MC-ICPMS. *Quat. Geochronol.* 1, 208–221. doi:10.1016/j.quageo.2006.08.002

Yang, H. J., Chen, Y. Q., Tian, J., Du, J. H., Zhu, Y. F., Li, H. H., et al. (2020). Great discovery and its significance of ultra-deep oil and gas exploration in well Luntan-1 of the Tarim Basin. *China Pet. Explor.* 25, 62–72. doi:10.3969/j.issn.1672-7703.2020.02.007

Yuan, H., Yin, S., Dong, L., and Tan, C. Q. (2022). Restoration of the pre-Jurassic paleogeomorphology and its control on hydrocarbon distribution in Western Ordos Basin. *Energy Geosci.* 4 (3), 485–494. doi:10.1016/j.engeos.2021.06.007

Zhang, Y. Q., Jia, J. D., Jin, J. Q., and Liu, Q. Y. (2007). Characteristics of cambrian-ordovician sedimentary facies in Tadong region and its sedimentary model. *Nat. Gas. Geosci.* 18, 229–234. doi:10.3969/j.issn.1672-1926.2007.02.014

Zhang, S. C., Zhang, B. M., Li, B. L., Zhu, G. Y., Su, J., and Wang, X. M. (2011a). History of hydrocarbon accumulations spanning important tectonic phases in marine sedimentary basins of China: Taking the Tarim Basin as an example. *Pet. Explor. Dev.* 38, 1–15. doi:10.1016/s1876-3804(11)60010-4

Zhang, S. C., Zhu, G. Y., Yang, H. J., Su, J., Yang, D. B., Zhu, Y. F., et al. (2011b). The phases of Ordovician hydrocarbon and their origin in the Tabei uplift, Tarim Basin. *Acta Petrol. Sin.* 27, 2447–2460.

Zhang, W., Guan, P., and Jian, X. (2014). Effects of Permian volcanic-magmatic activity on the Paleozoic oil and gas generating and storing conditions in the Tarim Basin. *Acta Sedimentol. Sin.* 32, 148–158. doi:10.14027/j.cnki.cjxb.2014.01.017

Zhang, G. Y., Liu, W., Zhang, L., Yu, B. S., Li, H. H., Zhang, B. M., et al. (2015). Cambrian-Ordovician prototypic basin, paleogeography and petroleum of Tarim Craton. *Earth Sci. Front.* 22, 269–276. doi:10.13745/j.esf.2015.03.023

Zhang, J. L., Feng, Z. H., Li, Q., and Zhang, B. (2018). Evolution of Cambrian mound-beach gas reservoirs in Gucheng platform margin zone. *Tarim. Basin. Pet. Geol. Exper.* 40, 655–661. doi:10.11781/sysydz201805655

Zhang, Y., Li, Q., Zheng, X. P., Li, Y. L., Shen, A. J., Zhu, M., et al. (2021). Cambrian-Ordovician platform type, evolution process and exploration potential in the Gucheng-Xiaotang area of eastern Tarim Basin. *Acta Pet. Sin.* 42, 447–465. doi:10.7623/syxb202104003

Zhao, M. J., Zhang, S. C., and Liao, Z. Q. (2001). The cracking gas from crude oil and its significance in gas exploration. *Petr. Explor. Dev.* 28, 47–56. doi:10.3321/j.issn:1000-0747.2001.04.014

Zhao, Z. J., Jia, C. Z., Zhou, X. Y., and Wang, Z. M. (2006). Key factors of oil-gas reservoir-forming and exploration targets in Ordovician in Tazhong area. *TarimBasin. China Pet. Explor.* 11, 6–16. doi:10.3969/j.issn.1672-7703.2006.04.002

Zhao, M. J., Zhang, S. C., Zhao, L., Liu, P. C., and Da, J. (2007). Geochemistry characteristics and Genesis of the paleoreservoir bitumen and natural gas in Nanpanjiang Basin. *Sci. China Ser. D. Earth Sci.* 37, 167–177. doi:10.3321/j.issn:1006-9267.2007.02.004

Zhao, Z. J., Zhang, Y. B., Pan, M., Wu, X. N., and Pan, W. Q. (2010). Cambrian sequence stratigraphic framework in Tarim Basin. *Geol. Rev.* 56, 609–620. doi:10.16509/j.georeview.2010.05.001

Zhao, W. Z., Shen, A. J., Hu, S. Y., Zhang, B. M., Pan, W. Q., Zhou, J. G., et al. (2012). Geological conditions and distributional features of large-scale carbonate reservoirs onshore China. *Petr. Explor. Dev.* 39, 1–14. doi:10.1016/s1876-3804(12)60010-x

Zhao, Z. J. (2015). Indicators of global sea-level change and research methods of marine tectonic sequences: Take ordovician of Tarim Basin as an example. *Acta Pet. Sin.* 36, 262–273. doi:10.7623/syxb201503002

Zheng, X. P., Zhang, Y., Chen, X. G., Yang, Z., Shao, G. M., and Bai, X. (2016). Natural gas exploration domains and analysis of carbonate reservoir characteristics in the east of Tarim Basin, NW China. *Nat. Gas. Geosci.* 27, 765–771. doi:10.11764/j.issn.1672-1926.2016.05.0765

Zhu, D. Y., Meng, Q. Q., Hu, W. X., and Jin, Z. Z. (2013). Differences between fluid activities in the central and north Tarim Basin. *Geochem.* 42, 82–94. doi:10.19700/j.0379-1726.2013.01.008

Zhu, G. Y., Chen, F. R., Chen, Z. Y., Zhang, Y., Xing, X., Tao, X. W., et al. (2016). Discovery and basic characteristics of the high-quality source rocks of the cambrian Yuertusi Formation in Tarim Basin. *Nat. Gas. Geosci.* 27, 8–21. doi:10.11764/j.issn.1672-1926.2016.01.0008